Biochimica et Biophysica Acta, 1150 (1993) 51–56
© 1993 Elsevier Science Publishers B.V. All rights reserved 0005-2736/93/$06.00

BBAMEM 76034

Human erythrocyte shape regulation: interaction of metabolic and redox status

Hoai-Thu N. Truong [1], David L. Daleke [2] and Wray H. Huestis

Department of Chemistry, Stanford University, Stanford, CA (USA)

(Received 15 April 1993)

Key words: Erythrocyte shape; Stomatocytosis; Dithiothreitol; Phospholipid asymmetry

The echinocyte-to-discocyte shape recovery of metabolically depleted erythrocytes is compromised by sulfhydryl reducing agents (Truong, H.-T.N., Ferrell, J.E., Jr. and Huestis, W.H. (1986) Blood 67, 214–221). In the presence of dithiothreitol (DTT) and sugars, crenated cells recover normal discoid shape transiently, but then develop the invaginations and intracellular inclusions of stomatocytes. The stomatogenic effects of DTT were investigated in erythrocytes recovering from crenation induced by several independent mechanisms. Cells crenated by direct manipulation of the membrane bilayer (lysophosphatidylcholine incorporation) recovered discoid shape similarly in the presence and absence of the reducing agent. In contrast, resealed ghosts and cells crenated by Mg^{2+} depletion or Ca^{2+} loading did not maintain stable discoid morphology in the presence of DTT, proceeding further to form stomatocytes. Thus cell crenation by expedients that involve cellular metabolic processes develop a redox-related morphological instability that is not found in amphipath-crenated cells.

Introduction

The normal functional human erythrocyte is a biconcave disc called a discocyte. In vitro, cell morphology can be manipulated to generate echinocytes (spiculate spheres) or stomatocytes (cupped discs or invaginated spheres) in what appear to be mirror-image processes. Methods for inducing such morphological changes may be divided into two categories: those that involve direct physical manipulation of the membrane lipid bilayer, and those that act indirectly through cellular biochemical processes.

Amphipaths appear to act by the first mechanism; negatively charged or net neutral agents such as phosphatidylcholine and pyrene butyric acid induce echinocytosis (also called crenation), while positively charged agents such as chlorpromazine produce stomatocytosis [1–4]. The differential action of amphipaths is consistent with the bilayer couple hypothesis [5], which attributes shape changes to buckling of the membrane due to preferential intercalation of the agents into the inner or outer leaflet of the lipid bilayer. Alternatively, the morphological action of certain inner monolayer intercalators has been attributed to changes in bilayer balance secondary to phospholipid scrambling [6]. In any case, such shape changes are reversed readily by removal or redistribution of the amphipaths.

Shape transformations also are effected by a range of experimental manipulations that, although their mechanisms are still in dispute, all seem to involve the metabolic machinery of the cell [7–12]. 'Metabolic' crenation (referring specifically to ATP depletion) is induced by incubating cells in the absence of nutrients [10,11]. Ca^{2+} crenation occurs when cells are loaded with calcium via an ionophore [12], a process distinct from ATP depletion [13]. Mg^{2+} depletion, induced by incubation with an ionophore and chelating agent, also crenates cells [14,15]. In these cases, crenation can be reversed by compensating for the injury: resuspension of ATP-depleted cells in nutrient rich buffer [10,16], elevation of intracellular magnesium [15], or removal of intracellular calcium [13], as appropriate, will restore discoid morphology.

In studies addressing the morphological effects of oxidative damage, we examined red cell recovery from ATP depletion in the presence of sulfhydryl reducing

Correspondence to: W.H. Huestis, Stanford University, Department of Chemistry Stanford, CA 94305, USA.

[1] Present address: Scios Nova, 2450 Bayshore Parkway, Mountain View, CA 94034, USA.

[2] Present address: Department of Chemistry, Indiana University, Bloomington, IN 47405, USA.

Abbreviations: CDTA, *trans*-1,2-diaminocyclohexane-*N,N,N',N'*-tetraacetic acid; DG, diacylglycerol; DTT, dithiothreitol, EGTA, ethyleneglycol-bis(β-aminoethyl ether)-*N,N,N',N'*-tetraacetic acid; LLPC, lauroyllysophosphatidylcholine; MI, morphological index; PS, phosphatidylserine, PE, phosphatidylethanolamine; PC, phosphatidylcholine.

agents [17]. Under conditions where control echinocytes recover to stable discoid morphology, dithiothreitol (DTT) and related reducing agents compromise shape regulation. In the presence of such agents and nutrients, crenated cells recover discoid shape transiently, but then evolve into stomatocytic and severely invaginated forms. The present study examines the molecular basis of this anomaly, comparing DTT effects on cell recovery from crenation induced by several independent mechanisms.

Materials and Methods

Materials. Penicillin G was obtained from Pfizer (New York), A23187 from Calbiochem-Behring (La Jolla, CA), and lucifierin-luciferase from LKB (Rockville, MD). All other biochemicals were obtained from Sigma (St. Louis, MO). Other chemicals were obtained from J.T. Baker (Phillipsburg, NJ) or Fisher Scientific (Pittsburgh, PA).

Cells. Human erythrocytes were obtained from healthy donors and isolated as described previously [17]. Cells were used within 3 h of being drawn. All incubations were carried out at 37°C in capped plastic tubes. For lengthy incubations, buffers contained 100 μg/ml streptomycin and 100 μg/ml penicillin (added as a 1000-fold concentrate) to retard bacterial growth.

Ghosts. Washed, packed erythrocytes were lysed and washed twice in 10 vols. cold 5 mM Na_2HPO_4 (pH 7.4 at 20°C), resuspended in 8 vols. of the same buffer containing 2 mM MgATP, and resealed by addition of 1 vol. 1.4 M KCl/0.2 M NaCl [7].

Lysophosphatidylcholine treatment. Cells were incubated at 37°C, 50% hematocrit, in a supplemented phosphate-buffered saline (138 mM NaCl, 5 mM KCl, 1.4 mM NaH_2PO_4, 6.1 mM Na_2HPO_4, 1 mM $MgSO_4$, 5 mM glucose (pH 7.4); plus 10 mM glucose, 10 mM inosine, and 1 mM adenosine) containing 0 or 0.2 mM lauroyllysophosphatidylcholine (LLPC). Under these conditions, all LLPC is incorporated into the cells within 2 min. After 2 min, DTT was added to yield a final concentration of 10 mM, and cell morphology was monitored as the function of further incubation time.

Ca^{2+}-loading and Mg^{2+}-depletion. Cells were depleted of magnesium by incubation at 37°C, 20% hematocrit, in high K^+ buffer (140 mM KCl, 5 mM NaCl, 5 mM glucose, 6.1 mM Na_2HPO_4, 1.4 mM NaH_2PO_4 (pH 7.4)) containing the ionophore A23187 (5 μM) and 1 μM EGTA. After 20 min, the solution was made 1 mM in CDTA. Shape recovery was initiated by addition of $MgSO_4$ to yield a concentration of 2 mM. CDTA and $MgSO_4$ were added as 100 mM stock solutions.

Calcium crenation was accomplished by suspending cells at 20% hematocrit in the above high K^+ buffer, also containing 400 μM $LaCl_3$, 250 μM $CaCl_2$, and 5 μM A23187. Suspensions were incubated at 37°C. After 20 and 25 min of incubation, additional increments of $CaCl_2$ (60 and 125 μM, respectively) were added. After 30 min incubation, cells were pelleted, washed by resuspension in phosphate-buffered saline, then allowed to recover discoid shape in the presence or absence of DTT. (A previous study [17] found that the degree of anomalous shape recovery in ATP-depleted cells depends on the reductant concentration, increasing up to a plateau above 6 mM DTT. This present work employs 10 mM DTT in all experiments.) Shape recoveries were achieved by incubation of cells at 37°C, 50% hematocrit, in phosphate-buffered saline plus 10 mM glucose, 10 mM inosine, and 1 mM adenosine. In the experiment described in Fig. 4, cells were treated as above, but the calcium loading buffer contained 10 μM A23187, 0.2 mM $LaCl_3$, 100 μM $CaCl_2$, 0.002% bovine serum albumin, and 0.28 mM $MgSO_4$. After 30 min incubation at 37°C, additional $CaCl_2$ was added (500 μM final concentration). At $t = 10$, 55, and 65 min, aliquots of cells were washed, resuspended in phosphate-buffered saline, and allowed to recover morphology in the presence or absence of DTT.

Morphology. Erythrocytes were fixed at 5% hematocrit in 150 mM NaCl containing 0.5% glutaraldehyde. Cells were examined by bright field microscopy at a magnification of 500×. Stomatocytes were assigned scores of −4 to −1, discocytes a score of 0, and echinocytes scores of +1 to +5, as described previously [10,15]. The average score for a field of 100 cells was called its morphological index (MI; 3). Multiple blind counts of replicate samples yields an experimental error on the order of 0.1 MI unit. The size of symbols in the figures represents this error range.

Shape change in resealed ghosts was quantified using a stomatocyte index. Echinocytic and discocytic ghosts were assigned a score of 0, and stomatocytic ghosts were scored −1 to −3, depending on the severity of invagination. Due to difficulty in distinguishing among severely stomatocytic ghosts, a stage −3 ghost corresponds to both −3 and −4 stomatocyte stages in intact cells.

Because of intrinsic variability in the quantitative morphological responses of cells derived from different donors, it is impractical to average results from multiple experiments. The data shown in figures represents the average of multiple samples analyzed in a single representative experiment.

ATP assays. ATP was assayed by the LKB luciferin-luciferase procedure.

Results

Shape recovery from LLPC crenation

Erythrocytes treated with 0.2 mM LLPC crenated within minutes (Fig. 1), then recovered discoid shape

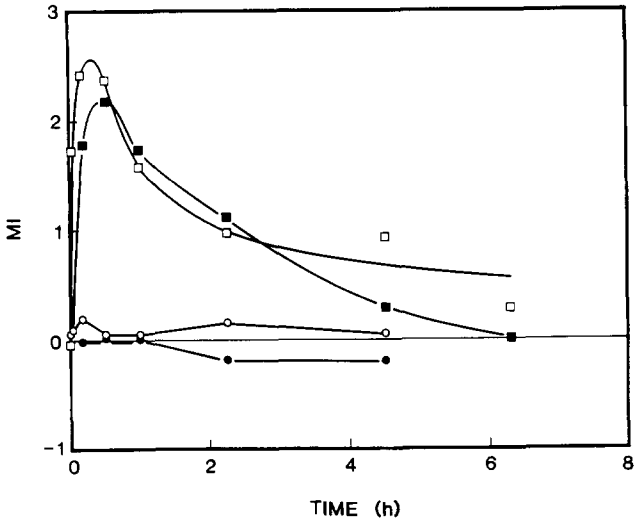

Fig. 1. DTT does not induce stomatocytosis in cells recovering from lysophosphatidylcholine crenation. Cells (50% hematocrit) were incubated at 37°C with 0 mM (○, ●) or 0.2 mM (□, ■) lysolauroylphosphatidylcholine. After 2 min, DTT was added (10 mM final concentration) to an aliquot of each sample (●, ■).

with a half-time of 3–4 h. DTT (closed symbols) accelerated the shape recovery slightly, but did not induce stomatocytosis.

Shape recovery from Mg^{2+}-depletion

Erythrocytes incubated with A23187 and chelating agents (1 μM EGTA plus 1 mM CDTA) crenated, forming stage 3 and 4 echinocytes within 2 h. Addition of excess $MgSO_4$ (2 mM) reversed the crenation: control cells reverted to discocytes, and cells treated identically in the presence of DTT became stomatocytic (Fig. 2). Both normal and exaggerated shape reversions proceeded with a half-time of 30 min.

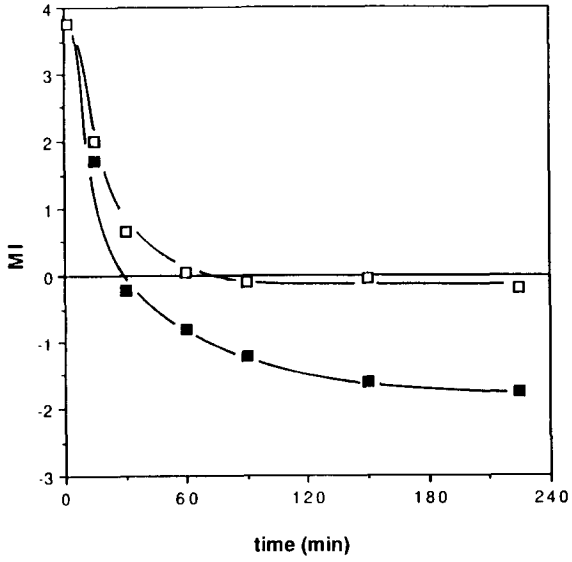

Fig. 2. DTT induces stomatocytosis in cells recovering from Mg^{2+} crenation. Cells (20% hematocrit) were incubated at 37°C in high K^+ buffer with 5 μM A23187 and 1 μM EGTA. After 20 min ($t = 0$), 1 mM CDTA was added; then $MgSO_4$ was added to yield 2 mM, and incubation was continued in the absence (□) or presence (■) of 10 mM DTT.

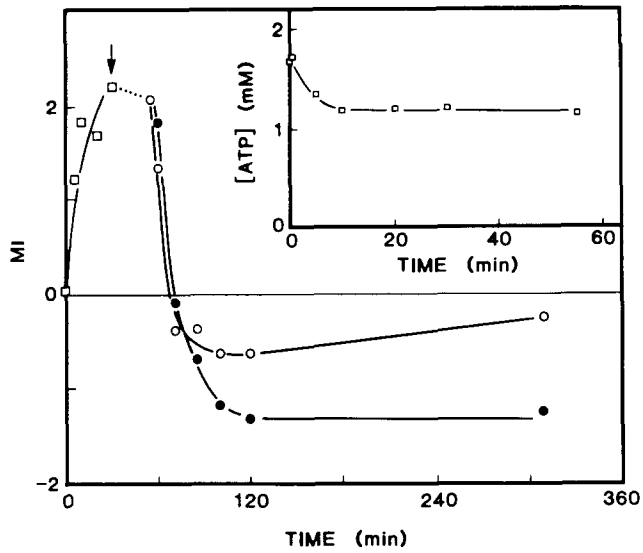

Fig. 3. DTT induces stomatocytosis in cells recovering from Ca^{2+} crenation. Cells (20% hematocrit) were incubated at 37°C in high K^+ buffer containing 400 μM $LaCl_3$, 250 μM $CaCl_2$, and 5 μM A23187 (●). Additonal increments of $CaCl_2$ were added at $t = 20$ (60 μM) and 25 (125 μM) min. At $t = 30$ min (arrow), cells were washed and resuspended in high K^+ buffer in the absence (○) or presence (●) of 10 mM DTT. (Inset) ATP levels during Ca^{2+} crenation.

Shape recovery from Ca^{2+}-loading

Erythrocytes were treated with calcium plus A23187 in high K^+/La^{+3} buffer (conditions that prevent cell shrinkage from calcium-induced potassium efflux, and that effect entry of calcium with minimal ATP depletion [18,19]). Within 30 min, cells exhibited an average morphology of +2.2 (Fig. 3). Cell ATP diminished, but remained above 1 mM (Fig. 3, inset). After 30 min the ionophore and exogenous calcium were removed. Upon further incubation at 37°C in phosphate-buffered saline, cells recovered discoid morphology and then assumed slightly cupped shapes (MI −0.7). Cells treated identically otherwise but allowed to recover in the presence of DTT became more severely stomatocytic, developing the invaginations typical of advanced stomatocytes (MI −1.4). The relationship between the severity of crenation and the eventual degree of DTT-induced stomatocytosis was examined (Fig. 4). Erythrocytes were loaded with first 100 μM and then 400 μM calcium, treatments that generated MI values of +2 and +3.3, respectively. Incubated in phosphate buffered saline, these cells reverted to normal discoid morphology. Treated with DTT in phosphate-buffered saline, the less severely crenated cells recovered to an MI of −1, while the more echinocytic cells became more severely stomatocytic (MI −1.6). Thus, the degree of DTT-induced stomatocytosis increased with the initial degree of crenation.

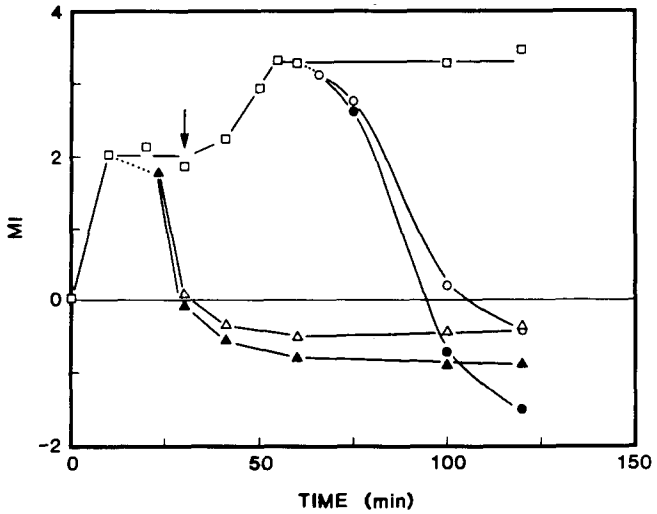

Fig. 4. The extent of DTT-induced stomatocytosis during recovery from Ca^{2+} crenation. Cells (20% hematocrit) were incubated at 37°C in high K^+ buffer with 10 μM A23187, 0.2 mM $LaCl_3$, 100 μM $CaCl_2$, 0.002% bovine serum albumin, and 0.28 mM $MgSO_4$ (□). At $t = 10$ min, an aliquot of cells was washed and resuspended in high K^+ buffer in the absence (△) or presence (▲) of 10 mM DTT. At $t = 40$ min (arrow), the remaining cells were supplemented with an additional 500 mM $CaCl_2$, incubated for 15 min, then washed and resuspended in buffer in the absence (○) or presence (●) of 10 mM DTT.

Shape changes in ghosts

Erythrocytes lysed in hypotonic, magnesium-free buffer [7], and then resealed around MgATP yield spiculate ghosts. When warmed to 37°C, such ghosts lose spiculate morphology, becoming stomatocytic [7,20]. When allowed to proceed in the presence of DTT, this stomatocytic transformation was more rapid and severe (Fig. 5).

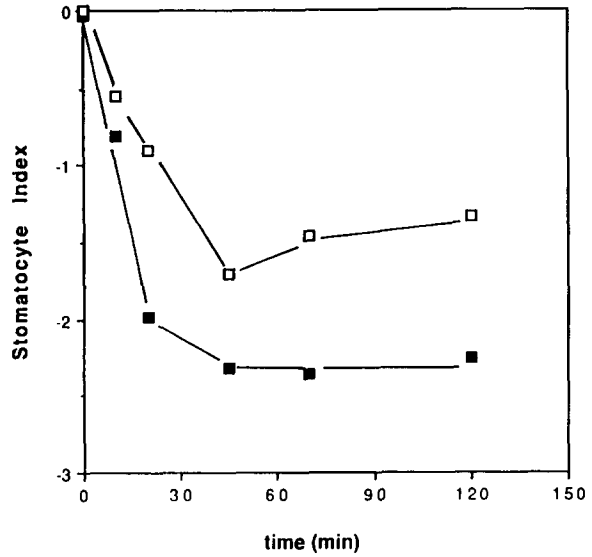

Fig. 5. DTT increases stomatocytosis in resealed ghosts. Ghosts prepared as described [7] were incubated at 37°C in the absence (□) or presence (■) of 10 mM DTT.

Discussion

DTT and other sulfhydryl reducing agents compromise erythrocyte morphology control in a complex manner: they have no evident effect on the shape of normal discocytes, but when added with nutrients, they cause ATP-depleted cells to evolve beyond discoid morphology to stomatocytes [17]. The redox status of erythrocytes appears linked to morphology control in other circumstances; oxidative damage has been implicated in the shape anomalies of metabolically depleted normal cells [21], hereditary spherocytic cells [22], and sickle cells [23]. In an attempt to identify the target(s) of oxidative sensitivity and the underlying link to metabolic control, the present studies examine the effects of sulfhydryl reduction on the shape recovery of echinocytes generated by four independent mechanisms.

DTT effects on amphipath-induced shape changes

LLPC crenates erythrocytes by insertion into the outer monolayer of the membrane, generating a transient stoichiometric imbalance between the phospholipid leaflets [24]. Cells crenated by lysolipid are morphologically distinct from metabolically crenated cells; the projecting spicules are finer and the population is more homogeneous. Cells recover rapidly from this type of crenation on reextraction of the foreign lipid [25], and revert spontaneously to discoid morphology as the exogenous lysolipid equilibrates slowly across the bilayer [26]. DTT treatment does not alter this spontaneous reversion significantly (Fig. 1); stomatocytosis is not observed. In a similar experiment, cells crenated by another outer monolayer intercalator, pyrenebutyric acid, recovered discoid shape normally in the presence or absence of DTT [27]. Thus, reducing agents do not affect shape recovery in cells crenated by direct manipulation of membrane bilayer balance.

DTT effects on magnesium- and calcium-dependent shape changes

In contrast, DTT has a marked effect on shape recovery from crenation induced by magnesium depletion or calcium loading. Magnesium-depleted cells attain an MI of +3.5 after 2 h incubation with magnesium chelators and ionophore; these echinocytes closely resemble cells crenated by metabolic starvation. Restoration of magnesium supports shape recovery to discocytes, which proceeds to stomatocytosis in the presence of DTT (Fig. 2). Cell ATP stores fall during magnesium depletion (data not shown), but the attendant shape change is unlikely to result directly from the ATP depletion. Crenation upon metabolic starva-

tion lags behind ATP depletion by 5–10 h [8,10], while in magnesium-depleted cells ATP depletion and crenation occur concurrently [28].

Calcium loading generates crenated cells that can recover discoid morphology upon removal of calcium. Again, in the presence of DTT the cells go beyond discoid to stomatocytic morphology (Fig. 4). Calcium crenation also is mechanistically distinct from echinocytosis due to ATP depletion [13]; the presence of lanthanum (an inhibitor of the Ca^{2+}-ATPase [19]) permits calcium loading without the exhaustive ATP depletion required for metabolic crenation (Fig. 3, inset).

(Control cells recovering from calcium loading also become sightly stomatocytic, though less so than cells recovering in DTT. This event may be due to membrane budding during the calcium treatment [29], which would decrease the outer-to-inner monolayer membrane balance.)

The stomatogenic effects of DTT also are evident in the shape changes of resealed erythrocyte ghosts. The ATP-dependent 'smoothing' reaction of ghosts is at best an approximation of shape changes of intact cells; unless medium Mg^{2+} levels are defined carefully, ghosts resealed around Mg^{2+}-ATP transform from spiculate to smooth to invaginated shapes, eventually forming spheres with endocytic inclusions [30]. This exaggerated shape recovery is accelerated and enhanced by DTT (Fig. 5).

Mechanistic correlations

The consistent effect of DTT on cells crenated by ATP depletion or by manipulation of cytosol ionic conditions suggests a common mode of action, beyond the level of bilayer stoichiometric balance, that links cell redox status to shape regulation. Several likely targets for such intervention may be eliminated on the basis of these studies, since the four crenation processes differ in mechanistic detail. Although all are associated with some reduction in ATP levels, in one case (calcium loading) the ATP decrease per se is inadequate to produce crenation, and in others (magnesium depletion, ghosts) the kinetics of crenation are inconsistent with starvation-induced echinocytosis. Crenation in intact cells and ghosts is associated with phosphoinositide degradation, but to different products, and lipid rephosphorylation processes are different during subsequent shape recoveries [10,31,32]. Further, DTT has no effect on lipid or protein phosphorylation during shape recovery from metabolic starvation [17]. Crenation by calcium loading and ATP depletion have been shown to be discrete processes that can proceed independently [13], with different effects on lipid and protein metabolism. Thus, specific action of DTT on an enzyme regulating phosphatidylinositide or protein phosphorylation cannot account for its general stomatogenic effect. Earlier work also showed that DTT has no effect on ATP synthesis or equilibrium cell glutathione levels in discocytes or recoverying echinocytes [17]. Although DTT-susceptible shape recoveries have in common a dependence on cell metabolic processes, lipid and protein phosphorylation and glycolysis are not likely to be the operant control mechanisms.

DTT effects on aminophospholipid transport

A possible target of reductive intervention is the phospholipid distribution in the plasma membrane. In erythrocytes, and in platelets and fibroblasts, choline lipids appear preponderantly in the outer membrane monolayer, while the amino phospholipids are confined primarily (phosphatidylethanolamine (PE)) or exclusively (phosphatidylserine (PS)) to the cytoplasmic monolayer. The aminophospholipid asymmetry is maintained by an active translocator [11,15,33,34] that transports both endogenous and exogenous aminophospholipids from the outer to the inner membrane monolayer. Such translocation requires ATP and magnesium and is inhibited by calcium and sulfhydryl oxidizing and alkylating agents [15,25,35,36]. DTT reverses the inhibition by sulfhydryl oxidants, both in erythrocytes [15,36] and in platelets [37].

Thus, conditions inhibiting aminophospholipid transport correlate significantly with conditions that dispose cells to DTT stomatocytosis. A possible mechanism of DTT action is interference with normal regulation of the lipid translocator. If DTT overcompensates for an oxidative lesion incurred by the transporter (during metabolic depletion, magnesium depletion, or calcium depletion), excessive transport of PE would be expected to produce stomatocytosis. This effect would be enhanced if transmembrane phospholipid asymmetry were lost during the crenating processes, as has been reported for metabolically depleted [38], or calcium loaded [39] cells and ghosts [40]. In that event, subsequent transport of PS and PE would be more rapid than return of choline lipids to the outer monolayer, and stomatocytosis would result. However, the extent to which lipids scramble under the above conditions is open to question; PS exposure is not detected in ATP-depleted cells assayed by the prothrombinase technique [41], which probably is less disruptive than the phospholipase treatment that suggested lipid scrambling [38].

Alternatively, a direct effect on the 'set point' of the translocator, such that the PE distribution is shifted more extensively toward the inner monolayer, could generate stomatocytosis without the necessity for lipid scrambling. Since DTT does not affect control cell morphology, such an effect would necessarily arise from events occurring during crenation. While subtle differences in the transbilayer distribution of PE are

not easily detected by available techniques, the effect of DTT on the general activity of the translocator is examined in experiments described in the accompanying manuscript [42].

Acknowledgements

This work was supported by the National Institutes of Health (HL23787). A portion of the work was carried out while H.-T.N.T. was a predoctoral fellow of the National Science Foundation.

References

1 Deuticke, B. (1968) Biophys. Biochim. Acta 163, 494–500.
2 Mohandas, N. and Feo, C. (1975) Blood Cells 1, 375–384.
3 Fujii, T., Sate, T., Tamura, A., Wakatsuke, M. and Kanaho, Y. (1979) Biochem. Pharmacol. 28, 613–620.
4 Alhanaty, E. and Sheetz, M.P. (1981) J. Cell Biol. 91, 884–888.
5 Sheetz, M.P. and Singer, S.J. (1974) Proc. Natl. Acad. Sci. USA 71, 4457–4461.
6 Shreier, S.L., Zachowshi, A. and Devaux, P. (1992) Blood 79, 782–786.
7 Sheetz, M.P. and Singer, S.J. (1977) J. Cell Biol. 73, 638–646.
8 Anderson, J. and Tyler, J.M. (1980) J. Biol. Chem. 225, 1259–1265.
9 Patel, V.P. and Fairbanks, G. (1981) J. Cell Biol. 88, 430–440.
10 Ferrell, J.E., Jr. and Huestis, W.H. (1984) J. Cell Biol. 98, 1992–1998.
11 Seigneuret, M. and Devaux, P.F. (1984) Proc. Natl. Acad. Sci. USA 81, 3751–3755.
12 Keuttner, J.F., Dreher, K.L., Rao, G.H.R., Eaton, J.W., Blackshear, P.L. and White, J.G. (1977) Am. J. Pathol. 88, 81–94.
13 Ferrell, J.E., Jr. and Huestis, W.H. (1982) Biochim. Biophys. Acta 687, 321–328.
14 Szasz, I., Hasitz, M., Breuer, J.H., Sarkadi, B. and Gardos, G. (1978) Acta Biol. Acad. Sci. Hung. 29, 1–17.
15 Daleke, D.L. and Huestis, W.H. (1985) Biochemistry 24, 5406–5416.
16 Nakao, M., Makao, T. and Yamazoe, S. (1960) Nature (London) 187, 945–946.
17 Truong, H.-T.N., Ferrell, J.E., Jr. and Huestis, W.H. (1986) Blood 67, 214–221.
18 Lew, V.L. and Ferreira, H.G. (1978) in Current Topics in Membranes and Transport (Branner, F. and Kleinzeller, A., eds.), Vol. 10, pp. 217–277, Academic Press, New York.
19 Sarkadi, B., Szasz, I. and Gardos, G. (1976) J. Membr. Biol. 26, 357–370.
20 Hayashi, H., Plishker, G.A., Vaughan, L. and Penniston, J.T. (1975) Biochim. Biophys. Acta 382, 218–229.
21 Palek, J., Liu, P.A. and Lin, S.C. (1978) Nature (London) 274, 505–507.
22 Becker, P.S., Morrow, J.S. and Lux, S.E. (1987) J. Clin. Invest. 80, 557–565.
23 Rice-Evans, C., Omorphos, S.C. and Baysal, E. (1986) Biochem. J. 237, 265–269.
24 Ferrell, J.E., Jr., Lee, K.J. and Huestis, W.H. (1985) Biochemistry 24, 2849–2857.
25 Daleke, D.L. and Huestis, W.H. (1989) J. Cell Biol. 108, 1375–1385.
26 Mohandas, N. and Feo, C. (1075) Blood Cells 1, 375–384.
27 Truong, H.-T.N. (1986) Ph.D. Thesis, Stanford University.
28 Daleke, D.L. (1986) Ph.D. Thesis, Stanford University.
29 Allan, D., Billah, M.M., Finean, J.B. and Mitchell, R.H. (1976) Nature (London) 261, 58–60.
30 Penniston, J.T. and Green, D.E. (1968) Arch. Biochem. Biophys. 128, 339–350.
31 Allan, D. and Thomas, P. (1981) Biochem. J. 198, 433–440.
32 Fairbanks, G., Patel, V.P. and Dino, J.E. (1981) Scand. J. Clin. Lab. Invest. 41, (Suppl. 156) 139–144.
33 Tilley, L., Cribier, S., Roelofsen, B., Op de Kamp, J.A.F. and Van Deenen, L.L.M. (1986) FEBS Lett. 194, 21–27.
34 Connor, J. and Schroit, A.J. (1987) Biochemistry 26, 5099–5105.
35 Zachowski, A., Faure, E., Cribier, S., Herve, P. and Devaux, P.F. (1986) Biochemistry 25, 2585–2590.
36 Connor, J. and Schroit, A.J. (1988) Biochemistry 27, 848–851.
37 Bevers, E.M., Tilly, R.H.J., Senden, J.M.G., Comfurius P. and Zwaal., R.F.A. (1989) Biochemistry 28, 2382–2387.
38 Haest, C.W.M. and Deuticke, B. (1975) Biochim. Biophys. Acta 401, 468–480.
39 Chandra, R., Joshi, P.C., Bajpai, V.K. and Gupta, C.M. (1987) Biochim. Biophys. Acta 902, 253–262.
40 Williamson, P., Algarin, L., Bateman, J., Choes, H.-R. and Schlegel, R.A. (1985) J. Cell. Phys. 123, 209–214.
41 Middelkoop, E., Van der Hoek, E.E., Bevers, E.M., Comfurius, P., Slotboom, A.J., Op den Kamp, J.A.F., Lubin, B., Zwaal, R.F.A. and Roelofsen, B. (1989) Biochim. Biophys. Acta 981, 151–160.
42 Truong, H.-T.T., Daleke, D.L. and Huestis, W.H. (1993) Biochim. Biophys. Acta 1150, 57–62.